Baseline

Long-term environmental changes in the Geum Estuary (South Korea): Implications of river impoundments

Sujin Kang [a], Jung-Hyun Kim [b,*], Young Jin Joe [b], Kwangchul Jang [b], Seung-Il Nam [b], Kyung-Hoon Shin [a,*]

[a] Hanyang University, ERICA campus, 55 Hanyangdaehak-ro, Sangnok-gu, Ansan-si, Gyeonggi-do 15588, South Korea
[b] KOPRI Korea Polar Research Institute, 26 Songdomirae-ro, Yeonsu-gu, Incheon 21990, South Korea

ABSTRACT

We investigated a sediment core collected from the Geum Estuary through sedimentological and geochemical analyses. Three lithological units were classified based on sedimentological characteristics. Unit 1 and Unit 3 were geochemically distinct, while Unit 2 was the transitional phase between them. The geochemical results suggest that the contribution of terrestrial organic carbon (OC) to the sedimentary OC pool in the coarse-grained Unit 1 was lesser than that of fine-grained Unit 3. The excess activity ($^{210}Pb_{ex}$) and the sedimentation rate indicate that Unit 1 corresponded to 1977 Common Era (CE). Since the first dam construction on the Geum River began in 1975 CE, the deposition of Unit 1 in the Geum Estuary is likely associated with river impoundments, which reduce the delivery of fine-grained sediment and terrestrial OC to the estuary. This study highlights the role of river impoundments in altering the sedimentary OC and thus the sedimentary environment in the estuary.

In the land-sea continuum, estuaries form when freshwater meets the sea in a semi-enclosed coastal body of water (Hobbie, 2000). They provide vital ecological services (Canuel and Hardison, 2016) and are often called the nurseries of the sea. Estuaries are important zones where terrestrial and marine organic carbon (OC) mix, which plays an important role in determining the OC fluxes to the adjacent coastal seas (Hedges and Keil, 1999; Canuel and Hardison, 2016). In the past century, river impoundments have been disturbing the natural OC delivery from land to sea (Bauer et al., 2013). Since the beginning of the twenty-first century, every year, 13% of the total organic carbon (TOC) carried by rivers is buried or remineralized in impounded reservoirs (Maavara et al., 2017), which significantly disrupts the river-to-sea OC transfer.

In South Korea, more than 17,000 dams including 1200 large dams and estuary dams have been constructed for freshwater supply, flood prevention, and recreation (Korea National Committee on Large Dams, KNCOLD, http://www.kncold.or.kr). Accordingly, river impoundments appear to have affected estuarine ecosystems such as phytoplankton communities, submerged macrophytes, mollusk growth, food web structure, and migratory shorebird populations (Hong et al., 2007; Sin et al., 2013; J.K. Lee et al., 2018; Son et al., 2018). Recently, issues about removal and opening of dams have been raised due to social interests in ecological restoration and environmental preservation (e.g., Koh and

Khim, 2014; Kim et al., 2016). Hence, studies to improve the understanding of carbon cycling within estuaries and assess potential changes in estuarine ecosystems upon removal or opening of dams are required.

The Geum River, which is the third largest river in South Korea, has a catchment area of 9914 km^2 and a length of 398 km (Water Resources Management Information System, WAMIS, http://www.wamis.go.kr). Its average annual discharge rate is 425 m^3 s^{-1} for the period of 2003–2018 (Water Environment Information System, WEIS, http://water.nier.go.kr). Since the construction of the Daecheong dam began in 1975, several multipurpose dams were built along the Geum River (Ahn et al., 2014). Two large dams (Daecheong and Yongdam) over 70 m high and three weirs (Sejong, Gongju, and Baekje) are in the upper- and mid-streams, respectively. Furthermore, an estuary dam was constructed in 1990. Based on the δ^{13}C and Δ^{14}C of particulate organic carbon (POC) in the surface water samples collected at the Geum Estuary in August 2016, Kang et al. (2020a) showed that phytoplankton-derived POC was the main contributor to the total POC pool in the reservoir of Geum Estuary. This study highlights that dams on the Geum River alter the source and reactivity of riverine POC, which could have been exported to the adjacent estuary when the water gate was open. However, such a study was based on a snapshot sampling strategy. Thus, information is still lacking about the impact of river impoundments on

the Geum Estuary over a longer period of time.

In this study, we investigated long-term environmental changes in the Geum Estuary by analyzing a sediment core through sedimentological (optical image, color, and grain size), organic (TOC, $\delta^{13}C_{TOC}$, and *n*-alkanes) and inorganic (radioisotopes, major and trace elements) analyses. Our aim was to determine the source of sedimentary OC and thus assess the long-term environmental changes associated with river impoundments.

In June 2018, we manually obtained a push core (GRC1, 115 cm length, 35°59.563′N, 126°36.455′E) in the tidal flat near Yubu Island, 13 km away from the Geum Estuary dam, using a PVC core barrel (Fig. 1). In the laboratory at the Korea Polar Research Institute (KOPRI), the sediment core was split, and described using the Munsell rock-color chart. After a visual inspection of the split core surfaces, optical image, color reflectance (L* and b*), and elemental composition were analyzed at KOPRI using an Itrax X-ray Fluorescence (XRF) core scanner at 5 mm resolution. The scanner was equipped with a Mo X-ray source operating at 30 kV and 30 mA with measurement times of 10 s. The color reflectance data contain L* describing the lightness between black (0) and

white (100), while b* denotes the yellow (positive values)–blue (negative values) chromaticity.

For grain size and geochemical analyses, the split core half that was not used for XRF measurement was subsampled at 5-cm intervals. For the grain size analysis at KOPRI, sediment samples were treated with 35% H_2O_2 to decompose organic matter. Then, sand-sized grains were separated from bulk sediments by wet sieving at 63 μm. The grain size for sediments smaller than 63 μm was measured using a Malvern Mastersizer 3000 laser particle size analyzer. For geochemical analyses, sediment samples were freeze-dried and homogenized. An aliquot of powdered sediment samples was added into a 6-mL counting tube to determine total ^{210}Pb and ^{226}Ra activities through well-type HPGe gamma spectrometry at the Korea Basic Science Institute (KBSI). Briefly, ^{210}Pb activity was measured by photopeaks at 46.5 keV and the photopeaks used for ^{226}Ra came from ^{214}Pb at 295.2 keV and 351.9 keV and ^{214}Bi at 609.3 keV (Kim and Burnett, 1983). TOC contents and $\delta^{13}C$ of the TOC ($\delta^{13}C_{TOC}$) were analyzed using an elemental analyzer combined with isotope ratio mass spectrometry at Hanyang University following the methods of Kang et al. (2019). The $\delta^{13}C$ values were calibrated using
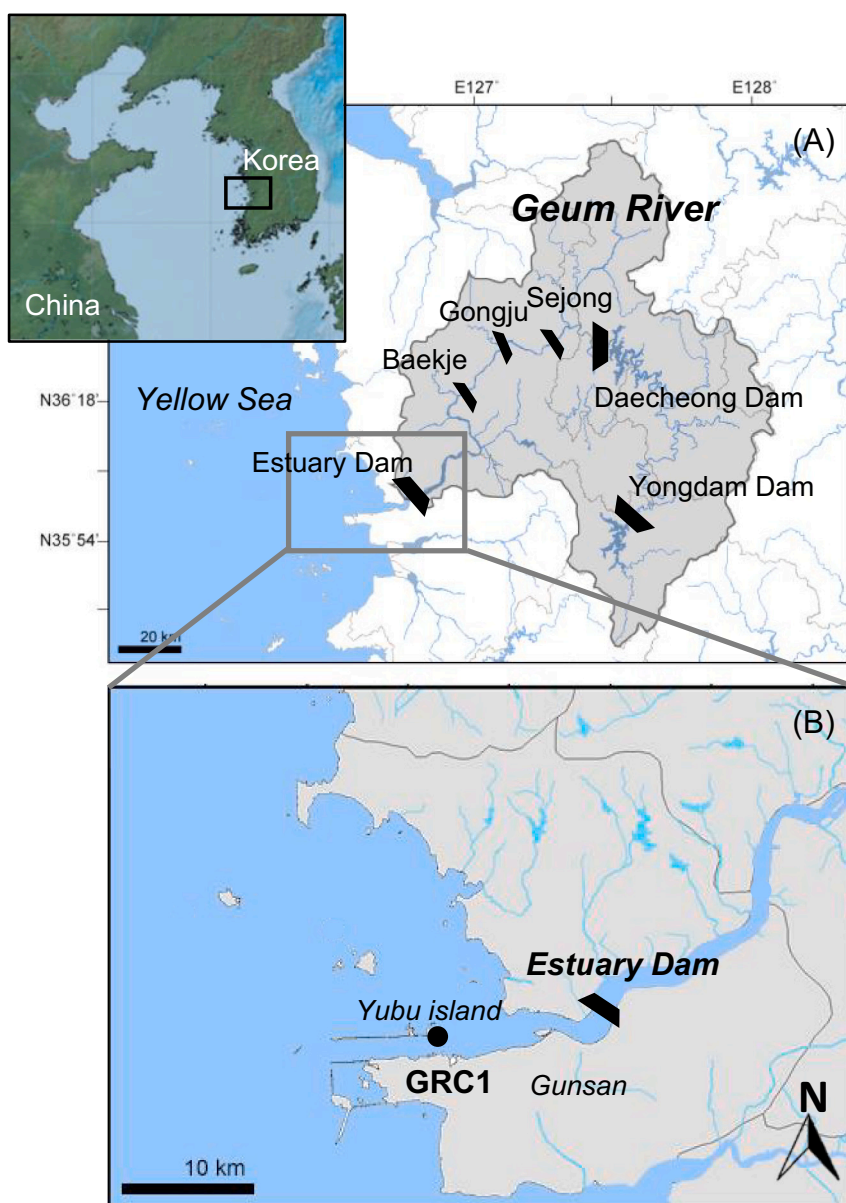
Fig. 1. (A) Map of the study area and (B) location of the studied sediment core (GRC1).

the IAEA-CH-3 standard with a $\delta^{13}C$ value of $-24.7‰$ certified by the International Atomic Energy Agency (Austria) and expressed by δ notation, relative to the standard Vienna Pee-Dee Belemnite for carbon (‰ VPDB).

Lipid extraction, purification, and analysis using an Agilent 7890A gas chromatography coupled with flame ionization detector (GC-FID) were conducted following the previously reported methods of Kim et al. (2017). S, Ti, and K concentrations were obtained using the Perkin Elmer Optima 4300DU inductively coupled plasma atomic emission spectrometry (ICP-AES) and Zr, Sr, Mn, Ni, and Cu concentrations were determined with the Thermo Elemental X-7 inductively coupled plasma mass spectrometry (ICP-MS) at KBSI following their standard procedures.

The lithology of core GRC1 is presented in Fig. 2 along with the core optical image, variations in color reflectance (L* and b*), grain size data (sand, silt, and clay contents), and core description. Core GRC1 was characterized by coarse upward sediments. Three lithological units were classified based on sediment color, texture, and structure. Unit 1, the upper 19 cm was the coarsest. This unit was composed of crudely laminated pale olive (5Y 6/3) and yellowish brown (2.5Y 6/3) sandy mud. The sand content was relatively constant (47 ± 6%). The silt and clay contents were in the range of 4–5% and 45–57%, respectively. The subsequent Unit 2 (19–65 cm core depth) was mostly massive dominated by yellowish brown (10YR 5/4) sandy mud with olive gray (5Y 3/2) mud clasts and was characterized as a slightly lighter and more yellowish color than Unit 1 (highest L* and b* values). Dark brown mottles were also partially observed. Brownish sediments contained higher sand contents, reaching up to 49%. The silt content increased at the bottom ranging between 45 and 78%, while the mud content was relatively constant between 5 and 8%. The grain size of this unit was fining towards the bottom, which was consistent with increased olive gray mud clasts. Below 65 cm core depth, Unit 3 was composed mainly of fine-grained mud characterized by dark olive gray color (lowest L* and b* values). Except for the core bottom, the grain size of this unit was generally constant with the dominance of silt fraction (79 ± 10%) and low sand and mud contents (less than 10%). In this unit, sub-parallel laminae were faintly recognized, and laterally discontinuous. Sediment color is an important parameter for delineating redox conditions of the sediments (Nagao and Nakashima, 1992). Variations in b* values are linked to the presence of high-valence iron oxides and hydroxides (Deaton and Balsam, 1991), which are prone to be enriched in oxidizing environments. Furthermore, fine-grained sediments increase the OC preservation due to reduced redox potential (Hedges and Keil, 1995). Hence, the light yellowish color of Unit 1 with high sand contents indicated that this unit was deposited under a more oxidizing condition than Unit 3.

The TOC contents and $\delta^{13}C_{TOC}$ values showed gradual changes along the core, ranging from 0.25 wt% to 0.74 wt% and from $-22.86‰$ to $-21.13‰$, respectively (Fig. 3). On average, the TOC was lower (0.30 ± 0.04 wt%) in Unit 1 than in Unit 3 (0.50 ± 0.10 wt%), while Unit 2 had intermediate values (0.37 ± 0.12 wt%). As generally shown in a positive relationship between the content of sedimentary OC and the surface area of sediments (Ransom et al., 1998), the highest TOC being in Unit 3 was associated with fine-grained muddy sediments with higher silt content (Fig. 2). In contrast, $\delta^{13}C_{TOC}$ values were on average slightly higher ($-21.6 ± 0.3‰$) in Unit 1 than in Unit 3 ($-22.6 ± 0.2‰$), whereas Unit 2 also had intermediate values ($-21.8 ± 0.3‰$). In general, terrestrial OC dominated by C_3 plants has depleted $\delta^{13}C$ values ($-32‰$ to $-24‰$) when compared to marine OC ($-24‰$ to $-16‰$) (Peterson and Fry, 1987; Meyers, 1994; Lamb et al., 2006; Marwick et al., 2015). Considering the fact that C_3 plants such as *Phragmites* spp. and *Salix* spp. are dominant in the Geum River watershed (S.-Y. Lee et al., 2018), Unit 1 with higher $\delta^{13}C_{TOC}$ values appears to have a lower proportion of terrestrial OC to the sedimentary OC pool than Unit 3. However, it should be noted that the $\delta^{13}C$ values of freshwater phytoplankton can be enriched depending on carbon sources used (Wang et al., 2013 and references therein). In the Geum River, the $\delta^{13}C$ of POC obtained in August 2016 was enriched with the value of $-19.4‰$, which was associated with the phytoplankton bloom (Kang et al., 2019, 2020b). Hence, riverine OC with enriched $\delta^{13}C$ values could transfer into the Geum Estuary and mask the $\delta^{13}C$ signatures of marine OC. Therefore, care should be taken when interpreting $\delta^{13}C$ values of sedimentary OC in this estuary system.

In order to better constrain sedimentary OC sources, we further analyzed the lipid biomarkers such as *n*-alkanes (Fig. 3). The resolved *n*-alkanes were detected in a series of C_{16} to C_{35} with the predominance of *n*-C_{29} and *n*-C_{31} homologues. The summed concentration of odd-carbon numbered high molecular weight (HMW) *n*-alkanes in the range of C_{25}–C_{31} ranged from 0.01–0.45 μg g^{-1}. The average chain length (ACL$_{25-31}$) (Cranwell et al., 1987) was 28.6 ± 0.2 and relatively stable.
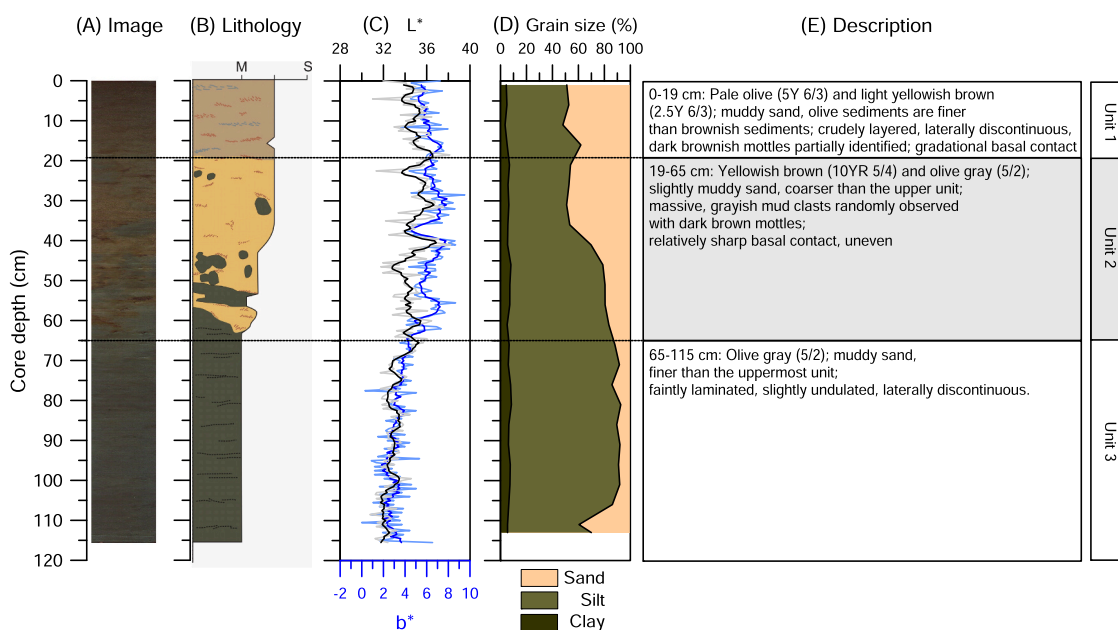
Fig. 2. (A) Optical image of core with (B) lithology, (C) variations in the color reflectance (L* and b*) and (D) grain size, including the content of sand, silt, and clay fractions, and (E) core description.
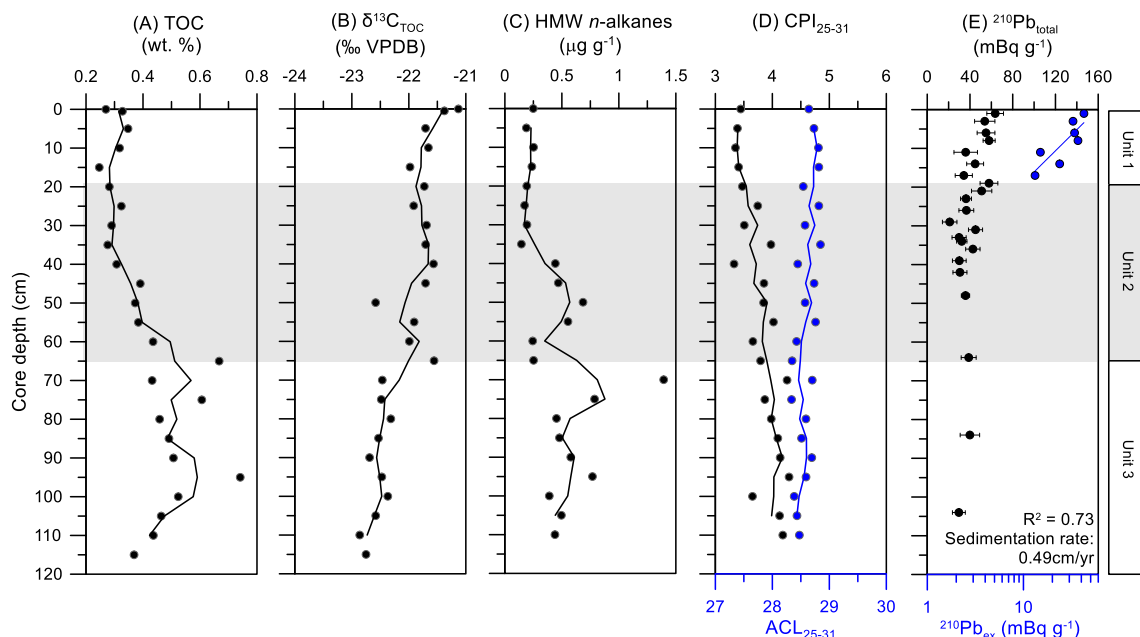
Fig. 3. Depth profiles of (A) total organic carbon (TOC), (B) carbon isotopic compositions ($\delta^{13}C_{TOC}$), (C) concentrations of high molecular weight (HWM) n-alkanes, (D) variations in CPI_{25-31} (black circles) and ACL_{25-31} (blue circles), and (E) $^{210}Pb_{total}$ (black circles) with the analytical error range and $^{210}Pb_{ex}$ (blue circles). (For interpretation of the references to color in this figure legend, the reader is referred to the web version of this article.)

The odd to even predominance of the n-alkanes, expressed as the carbon preference index (CPI_{25-31}) (Bray and Evans, 1961) was between 3.3 and 4.3. The odd-carbon numbered HMW n-alkanes ($>C_{25}$) are mainly derived from terrestrial vascular land plants, with maximum n-C_{27}, n-C_{29}, and n-C_{31} with CPI values of >4 (Cranwell et al., 1987; Eglinton and Hamilton, 1967; Mazurek and Simoneit, 1984; Meyers and Ishiwatari, 1993). Hence, the n-alkane maxima at n-C_{29} and n-C_{31} with the ACL_{25-31} of ~29 and the higher CPI_{24-32} value than 4 in Unit 3 are indicative of an origin predominant with epicuticular leaf waxes of higher land plants. The narrow range of ACL_{25-31} throughout the core also suggests that the source of HMW n-alkanes was relatively constant. Accordingly, the lower HMW n-alkanes concentrations in Unit 1 indicate that the

contribution of terrestrial OC to the sedimentary OC pool was lower in Unit 1 compared to Unit 3.

The Geum River supplies POC, clay minerals and associated elements as suspended loads to the estuary (Park et al., 1986; Wells and Park, 1992). Thus, we investigated changes in major and trace elements to determine the change in sediment sources. Because the XRF core scanning data is affected by factors such as uneven surface roughness of split sediments, mineral heterogeneities, changes in density, and surface grain size (Löwemark et al., 2019), we compared the scanning data with the element concentration data obtained from ICP-AES and ICP-MS based on the Spearman's correlation. Eight elements (S, K, Ti, Mn, Ni, Cu, Sr, and Zr) showed significant ($r_s > 0.5$, $p < 0.05$) correlations
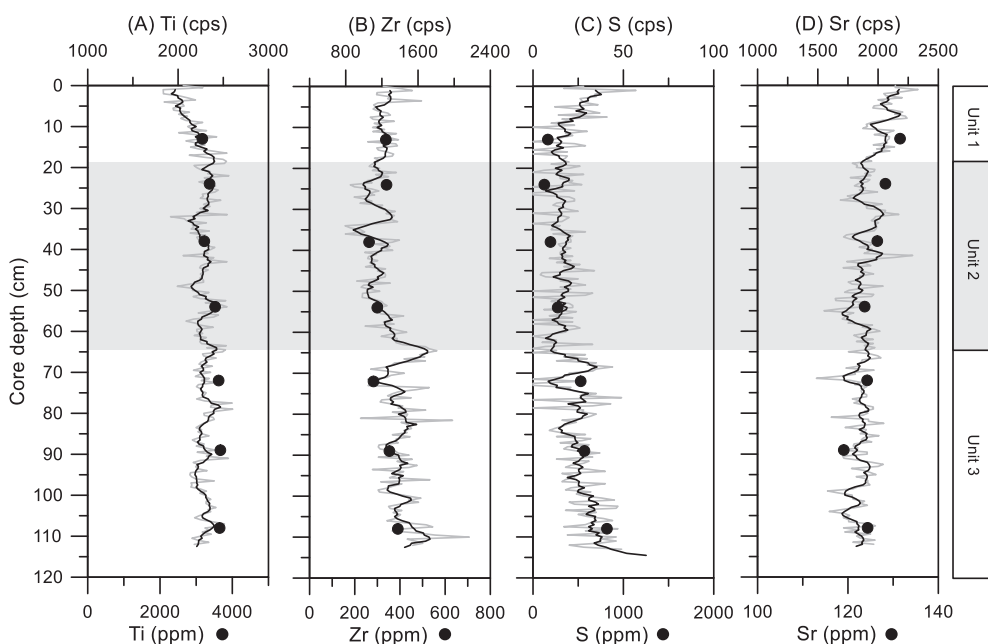
Fig. 4. Examples of comparisons between element count rates (cps) and concentration (ppm) datasets.

between the two datasets (Fig. 4). Among them, two elements (Ni and Cu) were excluded from further consideration due to their low concentrations (lower than 100 ppm). Note that Cl, indicating the effect of seawater (Vengosh et al., 1999; Dongmei and Matthew, 2018) was included for the principal component analysis (PCA) even though it was not quantified like other elements. For PCA, data were normalized by the auto-scaling method. The first two PCs had a cumulative percentage of 50% with eigenvalues higher than 1. The first principal component PC1 (29%) showed that marine-derived elements, Cl and Sr (Vengosh et al., 1999; Dongmei and Matthew, 2018), were positively loaded (Fig. 5A) whereas, Ti, a terrestrial-derived element (Goldberg and Arrhenius, 1958; Arz et al., 1998; Jansen et al., 1998; Jennerjahn et al., 2004; Chen et al., 2010), was negatively loaded (Fig. 5A). Accordingly, the relative contribution between terrestrial- and marine-derived elements governs PC1 as reflected by the highest Cl/Ti ratio in Unit 1 (Fig. 5B). Moreover, grain-size related elements such as Zr were positively loaded in the second principal component PC2 (21%). The Zr/Ti ratio is a variable related to the grain-size mineral fractionation, where Zr is relatively enriched in sand and medium to coarse silt minerals, while Ti is concentrated in finer minerals (Ishiga et al., 2000; Kylander et al., 2013; Taboada et al., 2006). For the core GRC1, the Zr/Ti ratios closely mimicked the variation in silt contents showing the highest value in Unit 3 (Fig. 2), suggesting that the PC2 was strongly related to the grain (especially silt) size of the sediments. Accordingly, Unit 1 contained higher seawater-derived elements in the sandy sediments than Unit 3.

To constrain the time frame of Unit 1, we analyzed $^{210}Pb_{total}$ and ^{226}Ra activities, which ranged between 21.0 and 63.6 mBq g^{-1} and 22.0–32.6 mBq g^{-1}, respectively (Fig. 3). The excess activities ($^{210}Pb_{ex}$) expressed as $^{210}Pb_{total}$ minus ^{226}Ra were between 11.6 and 35.6 mBq g^{-1} for Unit 1 (0–19 cm) and decreased logarithmically with depth. The estimated sedimentation rate was 0.49 cm yr^{-1} ($R^2 = 0.73$) for Unit 1, which based on the 19 cm of the core depth corresponded to roughly 1977 CE. Interestingly, the construction of the Daecheong dam on the Geum River began in 1975 CE. Hence, it is tempting to think that the deposit of Unit 1 is associated to the construction of the artificial structures along the Geum River. In general, dam constructions in midstream and estuary decrease the water discharge resulting in the accelerated accumulation of fine sediments in reservoirs, thereby decrease the supply of suspended loads to the estuary (e.g., Yang, 2014). In the case of the Geum River, 128 g m^{-3} of suspended loads were delivered to the estuary in 1985–1986 (Jeong et al., 2014), but the delivery of suspended, fine sediment loads to the estuary decreased to 42 g m^{-3} after increased river impoundments in 1994–2008 (Jeong et al., 2014). Therefore, the coarse, sandy-grained deposit of Unit 1 was likely associated with river impoundments, whereas the fine, silty-grained deposit of Unit 3 was accumulated under a more natural estuarine condition.

In summary, Unit 1 and Unit 3 showed distinct sedimentological and geochemical characteristics, while Unit 2 revealed a transitional phase between them. In brief, Unit 1 consisted of generally light yellowish coarse sediments (sandy with lower Zr/Ti ratios), whereas Unit 3 was mainly constituted of dark gray fine sediments (silty with higher Zr/Ti ratios). Unit I, when compared to Unit 3, showed lower TOC and HMW *n*-alkanes and higher $\delta^{13}C_{TOC}$ and Cl/Ti ratios. Accordingly, our sedimentological and geochemical data suggest that the contribution of terrestrial OC to sedimentary OC pool was reduced in Unit 1 compared to that in Unit 3. Thus, river impoundments along the Geum River appear to have reduced the delivery of terrestrial OC to the estuary, affecting the source of sedimentary OC and the sedimentary environment in the estuary. Further works are needed to evaluate long-term impacts of river impoundments on the estuarine ecology, by analyzing more sediment cores collected from different Geum Estuary areas.
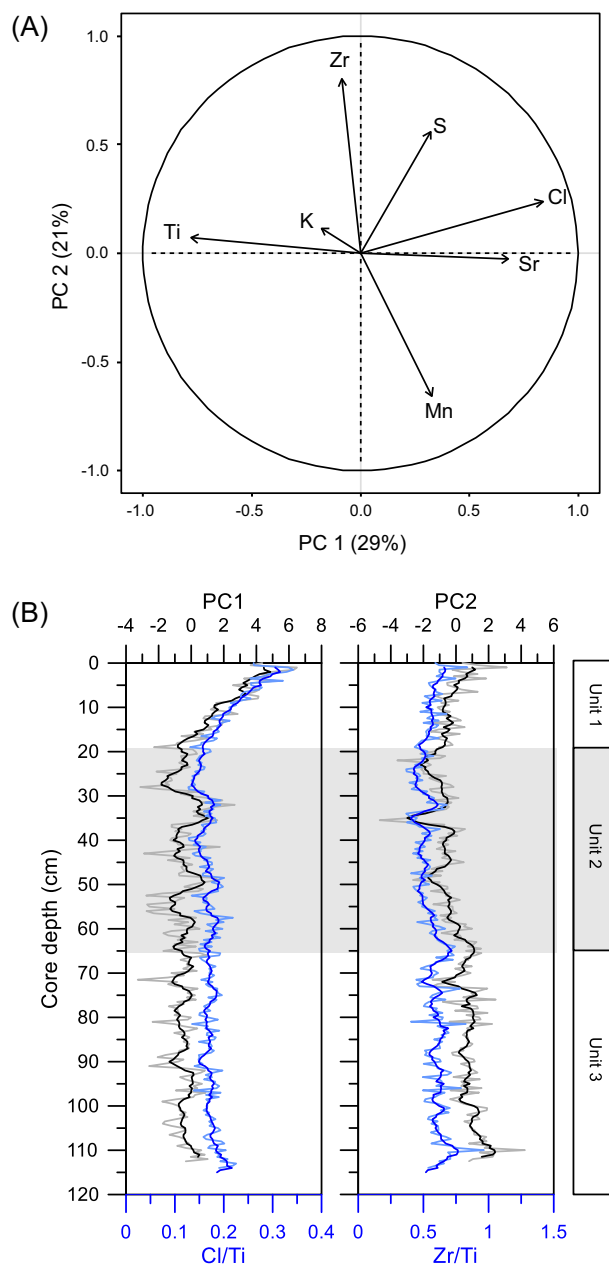
Fig. 5. (A) Results of the principal component analysis (PCA) and (B) depth profiles of PC1 and PC2 in comparison to Cl/Ti and Zr/Ti ratios.

CRediT authorship contribution statement

Sujin Kang: Conceptualization, Investigation, Writing – original draft. **Jung-Hyun Kim:** Conceptualization, Supervision, Writing – review & editing. **Young Jin Joe:** Investigation, Writing – review & editing. **Kwangchul Jang:** Investigation, Writing – review & editing. **Seung-Il Nam:** Writing – review & editing. **Kyung-Hoon Shin:** Supervision, Writing – review & editing.

Declaration of competing interest

The authors have no known competing financial interests or personal relationships that could influence the work reported in this paper.

Acknowledgements

References

Ahn, J.M., Lee, S., Kang, T., 2014. Evaluation of dams and weirs operating for water resource management of the Geum River. Sci. Total Environ. 478, 103–115. https://doi.org/10.1016/j.scitotenv.2014.01.038.

Arz, H.W., Pätzold, J., Wefer, G., 1998. Correlated millennial-scale changes in surface hydrography and terrigenous sediment yield inferred from last-glacial marine deposits off Northeastern Brazil. Quat. Res. 50, 157–166. https://doi.org/10.1006/qres.1998.1992.

Bauer, J.E., Cai, W.J., Raymond, P.A., Bianchi, T.S., Hopkinson, C.S., Regnier, P.A.G., 2013. The changing carbon cycle of the coastal ocean. Nature 504, 61–70. https://doi.org/10.1038/nature12857.

Bray, E.E., Evans, E.D., 1961. Distribution of n-paraffins as a clue to recognition of source beds. Geochim. Cosmochim. Acta 22, 2–15. https://doi.org/10.1016/0016-7037(61)90069-2.

Canuel, E.A., Hardison, A.K., 2016. Sources, ages, and alteration of organic matter in estuaries. Annu. Rev. Mar. Sci. 8, 409–434. https://doi.org/10.1146/annurev-marine-122414-034058.

Chen, H.-F., Song, S.-R., Lee, T.-Q., Löwemark, L., Chi, Z., Wang, Y., Hong, E., 2010. A multiproxy lake record from Inner Mongolia displays a late Holocene teleconnection between Central Asian and North Atlantic climates. Quat. Int. 227, 170–182. https://doi.org/10.1016/j.quaint.2010.03.005.

Cranwell, P.A., Eglinton, G., Robinson, N., 1987. Lipids of aquatic organisms as potential contributors to lacustrine sediments-II. Org. Geochem. 11, 513–527. https://doi.org/10.1016/0146-6380(87)90007-6.

Deaton, B.C., Balsam, W.L., 1991. Visible spectroscopy; a rapid method for determining hematite and goethite concentration in geological materials. J. Sediment. Res. 61, 628–632. https://doi.org/10.1306/D4267794-2B26-11D7-8648000102C1865D.

Dongmei, H., Matthew, J., 2018. Delineating multiple salinization processes in a coastal plain aquifer. Northern China: hydrochemical and isotopic evidence. Hydrol. Earth Syst. Sci. 22, 3473–3491. https://doi.org/10.5194/hess-22-3473-2018.

Eglinton, G., Hamilton, R.J., 1967. Leaf epicuticular waxes. Science 156, 1322–1335. https://doi.org/10.1126/science.156.3780.1322.

Goldberg, E.D., Arrhenius, G.O.S., 1958. Chemistry of Pacific pelagic sediments. Geochim. Cosmochim. Acta 13, 153–212. https://doi.org/10.1016/0016-7037(58)90046-2.

Hedges, J.I., Keil, R.G., 1995. Sedimentary organic matter preservation: an assessment and speculative synthesis. Mar. Chem. 49, 81–115. https://doi.org/10.1016/0304-4203(95)00008-F.

Hedges I., John, Keil G., Richard, 1999. Organic geochemical perspectives on estuarine processes: sorption reactions and consequences. Marine Chemistry 65, 55–65. https://doi.org/10.1016/S0304-4203(99)00010-9.

Hobbie, J.E., 2000. Estuarine science: the key to progress in coastal ecological research. In: Hobbie, J.E. (Ed.), Estuarine Science: A Synthetic Approach to Research and Practice. Island Press, Washington D.C, pp. 1–16.

Hong, J.-S., Yamashita, H., Sato, S., 2007. The Saemangeum reclamation project in South Korea threatens to extinguish an unique mollusk, ectosymbiotic bivalve species attached to the shell of *Lingula anatina*. Plankt. Benthos Res. 2, 70–75. https://doi.org/10.3800/pbr.2.70.

Ishiga, H., Nakamura, T., Sampei, Y., Tokuoka, T., Takayasu, K., 2000. Geochemical record of the Holocene Jomon transgression and human activity in coastal lagoon sediments of the San'in district. SW Japan. Glob. Planet. Change 25, 223–237. https://doi.org/10.1016/S0921-8181(00)00005-9.

Jansen, J.H.F., Van der Gaast, S.J., Koster, B., Vaars, A.J., 1998. CORTEX, a shipboard XRF-scanner for element analyses in split sediment cores. Mar. Geol. 151, 143–153. https://doi.org/10.1016/S0025-3227(98)00074-7.

Jennerjahn, T.C., Ittekkot, V., Arz, H.W., Behling, H., Pätzold, J., Wefer, G., 2004. Asynchronous terrestrial and marine signals of climate change during Heinrich events. Science 306, 2236–2239. https://doi.org/10.1126/science.1102490.

Jeong, Y.H., Yang, J.S., Park, K., 2014. Changes in water quality after the construction of an estuary dam in the Geum River estuary dam system. Korea. J. Coast. Res. 298, 1278–1286. https://doi.org/10.2112/JCOASTRES-D-13-00081.1.

Kang, S., Kim, J.H., Kim, D., Song, H., Ryu, J.S., Ock, G., Shin, K.H., 2019. Temporal variation in riverine organic carbon concentrations and fluxes in two contrasting estuary systems: Geum and Seomjin, South Korea. Environ. Int. 133, 105126. https://doi.org/10.1016/j.envint.2019.105126.

Kang, S., Kim, J.H., Ryu, J.S., Shin, K.H., 2020a. Dual carbon isotope ($\delta^{13}C$ and $\Delta^{14}C$) characterization of particulate organic carbon in the Geum and Seomjin estuaries, South Korea. Mar. Pollut. Bull. 150, 110719. https://doi.org/10.1016/j.marpolbul.2019.110719.

Kang, S., Kim, J.H., Hwang, J.H., Bong, Y.S., Ryu, J.S., Shin, K.H., 2020b. Seasonal contrast of particulate organic carbon (POC) characteristics in the Geum and Seomjin estuary systems (South Korea) revealed by carbon isotope ($\delta^{13}C$ and $\Delta^{14}C$) analyses. Water Res. 187, 116442. https://doi.org/10.1016/j.watres.2020.116442.

Kim, K.H., Burnett, W.C., 1983. γ-Ray spectrometric determination of uranium-series nuclides in marine phosphorites. Anal. Chem. 55, 1796–1800. https://doi.org/10.1021/ac00261a034.

Kim, D., Park, H., Park, S., 2016. The investigation of sea water intrusion length on opening of Nakdong River estuary barrage using numerical simulation model. Korean Soc. Hazard Mitig. 16, 299–309. https://doi.org/10.9798/kosham.2016.16.5.299.

Kim, J.H., Lee, D.H., Yoon, S.H., Jeong, K.S., Choi, B., Shin, K.H., 2017. Contribution of petroleum-derived organic carbon to sedimentary organic carbon pool in the eastern Yellow Sea (the Northwestern Pacific). Chemosphere 168, 1389–1399. https://doi.org/10.1016/j.chemosphere.2016.11.110.

Koh, C.H., Khim, J.S., 2014. The Korean tidal flat of the Yellow Sea: physical setting, ecosystem and management. Ocean Coast. Manag. 102, 398–414. https://doi.org/10.1016/j.ocecoaman.2014.07.008.

Korea National Committee on Large Dams, KNCOLD, n.d. http://www.kncold.or.kr (accessed 03 July 2020).

Kylander, M.E., Klaminder, J., Wohlfarth, B., Löwemark, L., 2013. Geochemical responses to paleoclimatic changes in Southern Sweden since the late glacial: the Hässeldala port lake sediment record. J. Paleolimnol. 50, 57–70. https://doi.org/10.1007/s10933-013-9704-z.

Lamb, A.L., Wilson, G.P., Leng, M.J., 2006. A review of coastal paleoclimate and relative sea-level reconstructions using $\delta^{13}C$ and C/N ratios in organic material. Earth Sci. Rev. 75, 29–57. https://doi.org/10.1016/j.earscirev.2005.10.003.

Lee, J.K., Chung, O.S., Park, J.Y., Kim, H.J., Hur, W.H., Kim, S.H., Kim, J.H., 2018a. Effects of the Saemangeum reclamation project on migratory shorebird staging in the Saemangeum and Geum estuaries. South Korea. Bird Conserv. Int. 28, 238–250. https://doi.org/10.1017/S0959270916000605.

Lee, S.-Y., Jang, R., Han, Y., Jung, Y., Lee, Soo-in, Lee, E., You, Y., 2018b. Health condition assessment using the riparian vegetation index and vegetation analysis of Geumgang mainstream and Mihocheon. Korean J. Environ. Ecol. 32, 105–117. https://doi.org/10.13047/KJEE.2018.32.1.105.

Löwemark, L., Bloemsma, M., Croudace, I., Daly, J.S., Edwards, R.J., Francus, P., Galloway, J.M., Gregory, B.R.B., Steven Huang, J.J., Jones, A.F., Kylander, M., Luo, Y., Maclachlan, S., Ohlendorf, C., Patterson, R.T., Pearce, C., Profe, J., Reinhardt, E.G., Stranne, C., Tjallingii, R., Turner, J.N., 2019. Practical guidelines and recent advances in the Itrax XRF core-scanning procedure. Quat. Int. 514, 16–29. https://doi.org/10.1016/j.quaint.2018.10.044.

Maavara, T., Lauerwald, R., Regnier, P., Van Cappellen, P., 2017. Global perturbation of organic carbon cycling by river damming. Nat. Commun. 8 https://doi.org/10.1038/ncomms15347.

Marwick, T.R., Tamooh, F., Teodoru, C.R., Borges, A.V., Darchambeau, F., Boillon, S., 2015. The age of river-transported carbon: a global perspective. Glob. Biogeochem. Cycles 29, 122–137. https://doi.org/10.1002/2014GB004911.

Mazurek, M.A., Simoneit, B.R.T., 1984. Characterization of biogenic and petroleum-derived organic matter in aerosols over remote, rural and urban areas. In: Keith, L.H. (Ed.), Identification and Analysis of Organic Pollutants in Air. Ann Arbor Science/Butterworth, Boston, USA, pp. 353–370.

Meyers, P.A., 1994. Preservation of elemental and isotopic source identification of sedimentary organic matter. Chem. Geol. 114, 289–302. https://doi.org/10.1016/0009-2541(94)90059-0.

Meyers, P.A., Ishiwatari, R., 1993. Lacustrine organic geochemistry-an overview of indicators of organic matter sources and diagenesis in lake sediments. Org. Geochem. 20, 867–900. https://doi.org/10.1016/0146-6380(93)90100-P.

Nagao, S., Nakashima, S., 1992. The factors controlling vertical color variations of North Atlantic Madeira Abyssal Plain sediments. Mar. Geol. 109, 83–94. https://doi.org/10.1016/0025-3227(92)90222-4.

Park, Y.A., Kim, S.C., Choi, J.H., 1986. The distribution and transportation of fine-grained sediments on the inner continental shelf off the Keum River estuary. Korea. Cont. Shelf Res. 5, 499–519. https://doi.org/10.1016/0278-4343(86)90073-7.

Peterson, B.J., Fry, B., 1987. Stable isotopes in ecosystem studies. Annu. Rev. Ecol. Syst. 18, 293–320. https://doi.org/10.1146/annurev.es.18.110187.001453.

Ransom, B., Kim, D., Kastner, M., Wainwright, S., 1998. Organic matter preservation on continental slopes: importance of mineralogy and surface area. Geochim. Cosmochim. Acta 62, 1329–1345. https://doi.org/10.1016/S0016-7037(98)00050-7.

Sin, Y., Hyun, B., Jeong, B., Soh, H.Y., 2013. Impacts of eutrophic freshwater inputs on water quality and phytoplankton size structure in a temperate estuary altered by a sea dike. Mar. Environ. Res. 85, 54–63. https://doi.org/10.1016/j.marenvres.2013.01.001.

Son, D., Cho, H., Lee, E.J., 2018. Determining factors for the occurrence and richness of submerged macrophytes in major Korean rivers. Aquat. Bot. 150, 82–88. https://doi.org/10.1016/j.aquabot.2018.07.003.

Taboada, T., Cortizas, A.M., García, C., García-Rodeja, E., 2006. Particle-size fractionation of titanium and zirconium during weathering and pedogenesis of granitic rocks in NW Spain. Geoderma 131, 218–236. https://doi.org/10.1016/j.geoderma.2005.03.025.

Vengosh, A., Spivack, A.J., Artzi, Y., Ayalon, A., 1999. Geochemical and boron, strontium, and oxygen isotopic constraints on the origin of the salinity in groundwater from the Mediterranean coast of Israel. Water Resour. Res. 35, 1877–1894. https://doi.org/10.1029/1999WR900024.

Wang, B., Liu, C.Q., Peng, X., Wang, F., 2013. Mechanisms controlling the carbon stable isotope composition of phytoplankton in karst reservoirs. J. Limnol. 72, 127–139. https://doi.org/10.4081/jlimnol.2013.e11.

Water Environment Information System, WEIS n.d., http://water.nier.go.kr (accessed 03 July 2020).

Water Resources Management Information System, WAMIS n.d., http://www.wamis.go.kr (accessed 03 July 2020).

Wells, J.T., Park, Y.A., 1992. Observations on shelf and subtidal channel flow: implications of sediment dispersal seaward of the Keum River estuary. Korea. Estuar. Coast. Shelf Sci. 34, 365–379. https://doi.org/10.1016/S0272-7714(05)80076-9.

Yang, J.S., 2014. Changed aquatic environment due to an estuary dam: similarities and differences between upstream and downstream. J. Korean Soc. Mar. Environ. Energy 17, 52–62. https://doi.org/10.7846/JKOSMEE.2014.17.1.52.